In vitro validation of measurement of volume elastic modulus using photoplethysmography

Haneen Njoum*, Panayiotis A Kyriacou

Research Centre for Biomedical Engineering, School of Mathematics Computer Science and Engineering, City, University of London, London, UK

ABSTRACT

Arterial stiffness (AS) is one of the earliest detectable symptoms of cardiovascular diseases and their progression. Current AS measurement methods provide an indirect and qualitative estimation of AS. The purpose of this study is to explore the utilisation of Photoplethysmography (PPG) as a measure of volumetric strain in providing a direct quantification of the Volume Elastic modulus (E_v). An *in vitro* experimental setup was designed using an arterial model to simulate the human circulation in health (*Model 2*) and disease (*Model 1*). Flow, pressure, and PPG signals were recorded continuously under varied conditions of flow dynamics. The obtained E_v values were validated with the gold standard mechanical testing techniques. Values obtained from both methods had no significant difference for both models with a percent error of 0.26% and 1.9% for *Model 1* and *Model 2*, respectively. This study shows that PPG and pressure signals can provide a direct measure of AS in an *in vitro* setup. With emerging noninvasive pressure measurement methods, this research paves the way for the direct quantification of AS *in vivo*.

1. Introduction

Cardiovascular diseases (CVD) are the foremost cause of death globally, with numerous risk factors such as diabetes, hypertension, hypercholesteremia, smoking and obesity associated with their development and progression [1–3]. Many studies have reported that the presence of these factors is related to a change in the mechanical properties of the arterial wall and an increase in Arterial Stiffness (AS) [4–8]. AS describes the reduced capability of an artery to expand and contract in response to pressure changes. Its clinical relevance is due to its fundamental role in pulsatile haemodynamic forces, as one of the earliest detectable symptoms of structural and functional changes within the vessel wall. AS is emerging as the most important determinant of increased systolic and pulse pressure in our ageing community. Therefore, AS is a root cause of cardiovascular complications at an early stage and is associated with accelerating Atherosclerosis (ATH) [9,10]. An increase in AS can be related to two major factors: (1) an increase in Intima Media Thickness (IMT) due to calcification, plaque formation, inflammation and rupture of elastin and collagen fibers [11,12]; (2) hypertension and hence an increase in the Circumferential Stress (CS) affecting the vessel wall which is associated with further cardiovascular complications and plaque rupture [13,14].

It is only recently that significant attention has been given to providing a precise measurement of AS. There has been an increased interest in the development of innovative non-invasive methods and devices for the diagnosis of CVD at an early stage in an effort to prevent further complications, and monitor pharmacological and non-pharmacological treatments [15,16]. In recent papers, we addressed the role of haemorheology in the photoplethysmographic waveform [17], and the relationship between the photoplethysmographic signal and transmural pressure values [18]. Further waveform analysis has been used for non-invasive estimations of AS [19–21].

Photoplethysmography (PPG), is a non-invasive optical technique commonly used for the measurement of arterial blood oxygen saturation in pulse oximetry [22]. It is widely accepted that the optical pulsations detected by a PPG system are modulated at the heart pulse rate due to arterial blood volumetric changes. The PPG signal, as is commonly referred, can be obtained at any vascular tissue surface using optical sensors, operating in either reflection or transmission mode [23,24]. The choice of the light sources used in pulse oximetry sensors varies between the visible and the near infrared range in accordance with the absorption spectra of oxy and deoxyhaemoglobin. The light transilluminates the tissue, and undergoes multiple stages of reflection, absorbance, and scattering. The photodetector, which is an integral part of the PPG sensor, captures the travelling light, where the current variations

* Corresponding author.

E-mail addresses: haneen.njoum.1@city.ac.uk (H. Njoum), p.kyriacou@city.ac.uk (P.A. Kyriacou).

are electronically processed, amplified and finally recorded. The PPG signal comprises two components, the pulsatile AC, and they non-pulsatile DC component. The origin of the signal and the question of what does PPG actually measures has attracted wide interest from the research community over the last decades [25–28]. Besides the major application of PPG in pulse oximetry, the signal is believed to contain further chemo-mechanical information related to the circulation [25,29,30]. For example, there were studies where the PPG was used to monitor blood pressure non-invasively [31–33]. Others have developed methods for the estimation of respiratory behaviour [34,35].

In relation to arterial stiffness, a host of indices derived from PPG and pulse pressure signals have been introduced to quantify AS [4,20,21,36–39]. When multiple indices exist, it is expected that none has proved any superiority, and all have problems in measurement and interpretation. Noninvasive measurement of AS entails measurement of parameters that are intrinsically associated with stiffness. The most widely used method is Pulse Wave Velocity (PWV), used for the estimation of AS by the Stiffness Index (SI) [21,40,41]. Further studies have explored the possibility of using the PPG pulse counter analysis and provide the augmentation index (AIx) [39,42]. AIx is the measure of the contribution that the wave reflection makes to the systolic arterial pressure, and is obtained by measuring the reflected wave coming from the periphery to the centre. It is defined as the ratio of the height of the late systolic peak to that of the early systolic peak in the pressure pulse. The second derivative of the PPG signal (SDPTG) has been utilised for the detection of the diastolic, systolic and inflexion points in the PPG for the estimation of arterial stiffness using AIx or the Reflection Index [21,43].

The PWV method measures the pulse propagation speed between two measurement sites. The parameter relevance to AS has been described in the late 19th century by Moens–Korteweg equation:

$$PWV = \sqrt{Eh/(2r\rho)} \tag{1}$$

and is determined by E, the *elastic modulus*, arterial geometry ($h =$ thickness, $r =$ radius) and blood density, ρ. The assessment involves measurement of two quantities: transit time of arterial pulse along the analysed arterial segment, and distance on the skin between both recording sites. A practical problem that arises in the measurement of PWV is when convenient points of measurement are not in the same line of travel. Moreover, inaccuracies are highly expected in determining the actual arterial distance between recording sites from measurements on the surface of the body [40]. PWV in large central elastic arteries such as the aorta increases markedly with age, whereas in upper limb arteries PWV does not increase. Furthermore, fundamental limitations still occur with PWV measurement due to ignoring some of the major variables in the circulation. Such factors include the pumping power of the heart, blood rheology, and the resistance of the microcirculation. All such factors are associated with changes in the thickness of the arterial wall (h), the arterial radius (r) and blood density (ρ), which will directly affect PWV, and hence a change in PWV might not necessarily reflect only stiffness changes in all cases [44–46].

Pulse pressure, pressure AIx and ambulatory arterial SI have been widely used in the identification of large AS. Over the age of 60 years, pulse pressure is expected to increase and is associated with a dominant rise in AS. However, in young subjects, pulse pressure increase at the peripheral site may lead to misinterpretations of hypertension. Thus, pulse pressure may not be a very accurate marker for assessing AS [47].

All indices suggested are known to be qualitative and indirect in principle. Clarenbach et al. reported a study comparing PPG with tonometry [20]. This study concluded that AIx and SI weakly correlated in patients with the chronic pulmonary disease or obstructive sleep apnoea. Such correlation was not observed at all when patients with low cardiovascular risk were included in the analysis. Moreover, AIx did not differentiate between patients with intermediate and high cardiovascular risks. Jerrard et al. demonstrated that in a hypertensive population, there was a poor agreement between PWV, AIx and pressure pulse methods. Following adjustment for age and gender, no correlation was observed [38]. Some other studies have shown IMT and PWV to be positively correlated, however, such relations were relatively weak and some studies have shown no relation [10,12]. Zureik et al. found no association in 564 subjects after adjusting for age and blood pressure [48]. Compared with the original reports there is sufficient evidence in the literature suggesting a poor correlation between those parameters in hypertensive patients whether treated or untreated, to the extent that all correlations were lost following adjustment for age and gender. The current understanding is that there is a disparity in the ability of these measures to predict future vascular events.

The *Volume Elastic modulus* (E_v) is estimated from the regional Pressure–Volume (P–V) relationship. This parameter provides comprehensive information on the arterial wall properties regarding the global effect of the circulation. A higher value of E_v suggests increased stiffness. Currently, there are no studies in the literature reporting on the precise and direct measurement of E_v of the arterial wall using non-invasive methods.

In this study, we have developed a new method to measure E_v using the PPG and pressure signals. We validated the method in an *in vitro* model of human circulation in health and disease. During an *in vivo* scenario, many factors can influence the dynamics of the flow. This includes the vassal tone, the specific biochemical content, and the endothelial activity. Such factors also vary from one participant to another and can be altered in the same participant throughout the day. To overcome some of these limitations and develop a better understanding of the quantitative analysis of the PPG, an *in vitro* setup was developed. This allowed validation of the proposed method with the gold standard elasticity method of extension testing and generating the true stress-strain curve, a merely unfeasible practice for *in vivo* studies. In this paper, we present *in vitro* results, highlighting the capability of using the PPG components as a measure of AS which could contribute further in the diagnosis of complications related to biomechanical abnormalities in the arterial wall and the endothelium.

1.1. Theoretical method

Consider a circular tube with an initial volume (V_1); suppose the inner surfaces of the tube are exposed to transmural pressure (P); forces of radial stress are perpendicular to and act on all surfaces uniformly as seen in Fig. 1(a). The response of the object to this uniform stress is an expansion of volume to V_2. This behaviour can be characterised using the bulk modulus or the Volume Elastic modulus (E_v) which can be expressed with the following relationship:

$$\left(\frac{dV}{V}\right).E_v = dP \tag{2a}$$

where dP, is the change in the transmural pressure signal, and dV is the change in the volumetric signal. In the presence of pulsatile flow conditions, the side view of the tube can be represented as seen in Fig. 1(b) and the pulsatile transmural pressure (P) and Volume (V) signals are out of phase (∅), as seen in Fig. 1(d). Due to the time-dependency of the pulsatile flow, Eq. (2a) can be derived with respect to time and expressed with Eq. (2b). This is illustrated in the linear approximation in Fig. 1(c). Here, the flow is assumed
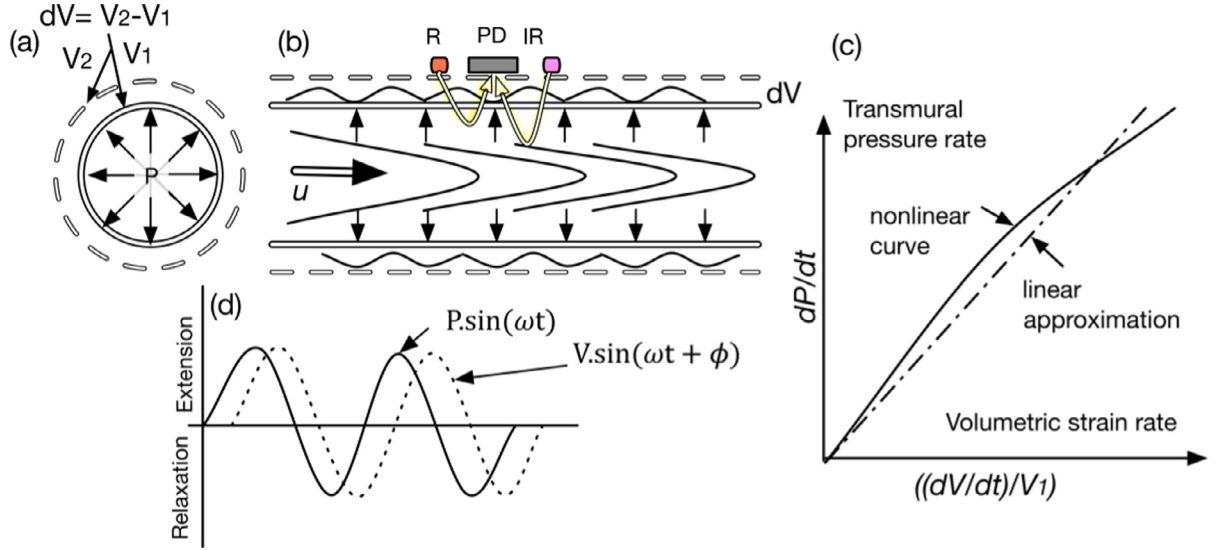
Fig. 1. (a) Cross-sectional view of flow in a cylindrical model. (b) Side view of flow in a the model with a pulsatile pressure signal. (c) is a representation of the nonlinear curve and the linear approximation for measurement of Elastic Volume Modulus (d) the relationship between the pulsatile pressure and the pulsatile strain signals, where w, is the radian frequency, and is the phase between both signals.

to have an oscillating time-dependent volumetric signal dV and a steady flow volume V, the constant volume of the steady flow that develops at the centre of the tube.

$$E_v = d(dP/dt)/d((dV/dt)/V) \tag{2b}$$

1.2. Measurement of volumetric strain

The volumetric strain in the arterial model was measured using the PPG signals. We consider the pulsatile flow to consist of an oscillatory component ($\tilde{V}_o$) and a steady component ($\tilde{V}_s$) [49]. Assuming that the Beer–Lambert 's Law holds in this model, the following equation expresses the relation between the total incident (I_0) and total transmitted light (I) [19,50]:

$$I = \exp\left(-\varepsilon_s c_s \bar{V}_s\right)\exp\left(-\varepsilon_o c_o \tilde{V}_o\right)I_0 \tag{3}$$

where c is the concentration of the light-absorbing substance in each component and ε is the absorbance coefficient. The subscripts, o and s, denote oscillatory and steady components respectively. Given that ($\bar{V}_s$) is constant at the same pressure and wall elasticity, the following equation holds for the steady volume component:

$$\bar{I} = \exp\left(-\varepsilon_s c_s \bar{V}_s\right)I_0 \tag{4}$$

where, ($\bar{I}$) is constant light intensity obtained from the steady volume layer.

Hence, from (3) and (4), and by deriving both sides in respect to time, the following can be derived

$$\tilde{V}_o = -\varepsilon c.ln(I/\bar{I}) \tag{5}$$

considering that dI is the amplitude of the oscillatory optical signal, and $\bar{I}$ is the level of the steady optical signal, at a particular wavelength. It is noted that $\ln(I/\bar{I})$ is in direct proportion to the oscillatory component of the total fluid volume ($\tilde{V}_o$), via the unknown constant term ($\varepsilon_o c_o$), presuming that both are constant Normalised Pulse Volume (NPV) can be given by

$$NPV = -ln(dI/\bar{I}) \tag{6}$$

as we are interested in the behaviour of a time-dependent signal, deriving (6) in respect to time and relying on the assumption that

($\varepsilon_o c_o$) is an unknown constant term, the rate of change of NPV would be

$$(dNPV/dt) = -(dI/dt)/I \tag{7}$$

finally, we introduce the rate of change of Normalised Volumetric Strain (NVS) as $dNPV/dt/NPV$ which is given by the following equation:

$$dNVS/dt = (dI/dt)/I.\ln(dI/\bar{I}) \tag{8}$$

considering that there is no change of volumetric strain when the rate of change of pressure is zero then E_v from Eq. (2b) can be expressed as in Eq. (9)

$$E_v = (dP/dt)/(dNVS/dt) \tag{9}$$

1.3. Objectives

In order to investigate the plausibility of utilising the PPG components and pressure signals for the quantification of tissue mechanical properties, an *in-vitro* experiment was conducted with an aim to:

- Evaluate the feasibility of the new method for direct measurement of E_v in an *in vitro* model featuring a healthy artery and another affected with ATH. This is achieved by collecting PPG and pressure signals and validate the results with the gold standard E_v measurements.
- Investigate E_v values over a range of pressure values in normotensive, hypotensive and hypertensive conditions by controlling the stroke volume and pulse frequency.
- Contribute to the further understanding of the behaviour of the PPG in pulsatile flow considering the wall elastic properties and flow dynamic forces.

2. Materials and methods

An *in vitro* study was carried out to investigate PPG pulsatile signals (AC) under different scenarios of flow dynamics. The *in vitro* experimental setup, described in the following subsections was designed to simulate the flow conditions observed in the human circulation.
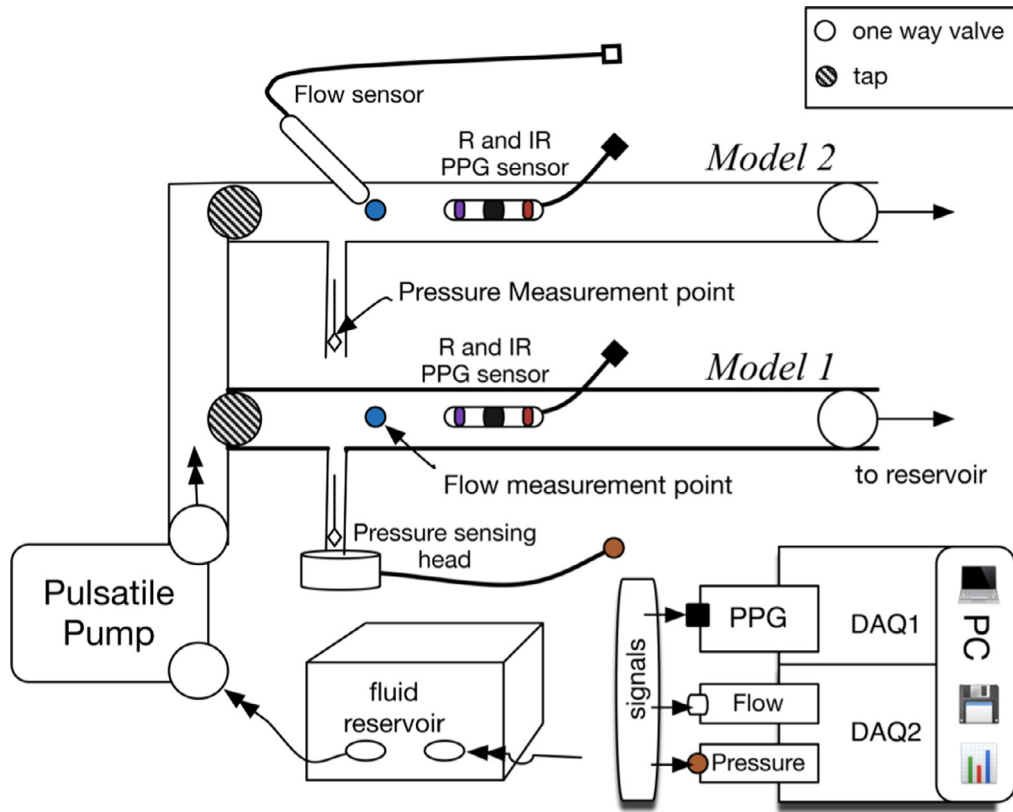
Fig. 2. A schematic diagram of the flow loop used to impose mechanical stress at variable flow patterns.

2.1. The arterial network model

A pulsatile flow loop illustrated in Fig. 2 was designed to contain an elaborate elastic tubes model and produce a range of patterns of mechanical forces at the inner surface of the elastic tubing. A pulsatile pump (1423 PBP, Harvard Apparatus, US) was used to generate the pulsatile flow. The pump allowed control of flow by two means (1) controlling the stroke volume (2) and the pumping rate. A custom made plexiglass fluid reservoir (Volume: 8 L) was developed to contain the fluid for the circulation.

A flexible Polyvinyl Chloride (PVC) tubing at a length (L) of 20 cm, Wall Thickness (WT) of 3 mm and an Inner Diameter (ID) of 16 mm was connected to the input of the system to enable the flow to be fully developed before entering the model. The model consisted of two different elastic transparent tubes with different elasticities. The purpose of the two elastic tubes is to simulate the change from healthy arteries to an advanced stage of ATH with reduced elasticity and increased wall thickness The setup consisted of two tubes (L: 30 cm): (1) *Model 1* consisted of a PVC tube (ID: 16 mm, WT: 1.8 mm) which simulates a large artery affected with ATH, with increased IMT and AS; (2) *Model 2* is a silicone rubber tube (ID: 16 mm, WT: 0.9 mm) which simulates a healthy artery.

The model was mounted onto a custom made support system which incorporated rubber clamps to hold the tubes straight at a constant length without interfering with their movement. An initial axial stretch of 1–2% was used to ensure that the flexible tubes remained in a straight position during the pumping phase. One-way check valves with preset opening pressure (50 mmHg) were introduced at both ends of each tube which provided the control over the resistance and backward flow. Valves were also introduced at the entrance of each tube to allow control of flow paths and switch to a bypass tube in order to eliminate any bubbles in the
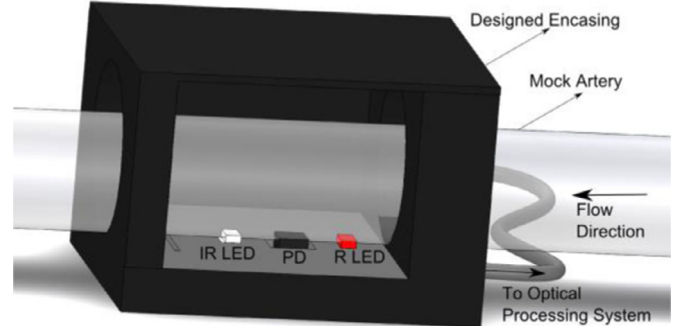

Fig. 3. 3D illustration of the custom-made PPG optical sensor enclosing a tube section, showing Infrared (IR) and Red (R) LEDs, a photodiode (PD), mock artery and the designed encasing.

system. The room temperature during all *in vitro* experiments was maintained at 23±0.5°C.

2.2. Sensors and instrumentation

2.2.1. PPG sensor

The reflectance photoplethysmography sensor used was designed and fabricated in the laboratory. Two LEDs, Red (R) and Infrared (IR), at peak wavelengths of 640 nm and 860 nm respectively, were aligned in a reflectance mode at a 3 mm distance from the photodiode (PD) (Vishay, UK). A 3D printed (MakerBot, US) encasing was fabricated to fix the probe at a 1 mm contact gap with the pulsating tube without interfering with its motion. A 3D model of the designed PPG probe and encasing is illustrated in Fig. 3.

2.3. Pressure and flow measurement

The pressure was measured at the entrance of each tube using a catheter tip research grade transducer (Harvard Apparatus, U.S.) inserted through the lumen of the model. The flow rate was measured at the centre of each tube using an ultrasound Doppler (MD2, Huntleigh Healthcare, UK) with an 8 MHz probe. A 3D printed holder was also designed to hold the probe at a 60 ∘ angle with the tube without interfering with the tube's wall motion.

2.4. PPG processing system and data acquisition

For the acquisition of PPG signals, a custom-made two-channel dual wavelength PPG instrumentation system was designed for this study. The PPG processing system was constructed to pre-process and convert the detected current into voltages for later acquisition. The processing system used multiplexed current sources (set to 25 mA) to drive both red and infrared LEDs consecutively. The microcontroller generates the digital switching clock so that the photodetector captures both at a frequency of 900 Hz. The mixed signals were fed into the demultiplexer and were then split into their respective red and infrared PPG signals. The PPG signals were then low-pass filtered at a cut-off frequency of 40 Hz and amplified with a gain of 19. The processed pressure signals were digitised using the 9172-c Data Acquisition card (DAQ2) (National Instruments, UK). The processed red and infrared AC and DC PPG signals were digitised using a National Instruments PCIe-6321 16-bit data acquisition card (DAQ1) (National Instruments Inc., Austin, TX, USA). All signals were digitised at a sampling rate of 1 kHz and were recorded for further offline analyses.

2.5. Fluid handling

Extra pure hexahydrate Cobalt (II) Nitrate powder $Co(NO_3)_2$ (Fischer Scientific, UK) was prepared with a saline solution to produce 2 L of a 0.6 mol/L solution. The fluid optical properties were measured in the visible and near infrared region using a spectrophotometer (Lambda 1050, Perkin Elmer). The fluid viscosity was measured at shear rates of 40, 60 and 90 rpm using a cone/plate viscometer LVD3T (Brookfield, US). pH and conductivity measurements were obtained using the pH/conductivity meter (Jenway, UK)

2.6. In vitro experimental protocol

In order to evaluate the plausibility of using the PPG and pressure signals in the identification of arterial stiffness, *Model 1* and *Model 2* were tested under varying patterns of fluid dynamic forces. Flow rates were controlled by adjusting the pump to operate for 10 min at each pumping frequency representing a heartbeat of 40, 60 and 90 bpm.

Flow rates were also controlled by adjusting the stroke volume at 30 ml and 70 ml. At each stroke volume, the pump was also adjusted to pump at the three different pulse frequencies (40, 60, 90 bpm). Systolic to diastolic pumping ratios were maintained at 25%−75%. To avoid any inaccuracies, a bubble-free flow and a steady pulsatile pattern were maintained. The designed model allowed bypassing any trapped bubbles and adjustment of pressure limits by using the one-way check valves installed at each model and stopcocks at the entrance for each model.

2.7. Data analysis

2.7.1. Gold standard measurement of e

The *elastic modulus* (E) for both tube models was tested using the stress-strain curve from the gold standard method. The gold

Table 1
Fluid viscosity measurement.

Shear rate (rpm)	Viscosity (mPa.s)
40	3.73
60	2.78
90	1.39

standard is a calibrated electromechanical system Instron (model 5900, Instron Co, USA). A 100 mm specimen from each tube was extended at a rate of 0.1 mm/s to obtain the stress-strain curve. E is calculated from the slope measurement of that curve. v is Poisson's ratio and is estimated from the traverse-longitudinal strain curve. E_v was calculated from the relationship $E = 3E_v(1 - 2v)$.

2.7.2. Proposed method for pulse analysis for measurement of E_v

The offline analysis was performed using automated software developed in Matlab (Mathworks, Inc. Natick, MA). PPG signals were filtered accordingly to provide the AC and DC components. Peaks and valleys of PPG and pressure signals were detected using a custom-made peak detector script using the first and second derivative. Pressure and optical rate of change in respect to time was performed on 30% of the signal in the systolic region as seen in Fig. 4. This region was chosen to standardise the measurement at different stroke volumes and frequencies. It is the region that mostly contributes to the changes in wall stiffness and it was purposely selected in order to reduce the contribution of fluid properties and resistance that will be mostly observed in the lower region of the systolic phase. The change rate of NVS was obtained from the PPG signals as described in Eq. (8). To avoid inaccuracies, the measurement extended from 60% to 90% before the peak. Finally, Eq. (9) can be rewritten as seen in Eq. (10) and E_v can be calculated as follows:

$$E_v = (\Delta P_{d,c}/\Delta t_{d,c})/\left(\left(\left(\Delta I_{b,a}/\Delta t_{b,a}\right)/\left(I_a.\ln\left(\Delta I_{pk-pk}/\overline{I}\right)\right)\right).K\right) \quad (10)$$

where a,b,c,d are denoted as seen in Fig. 4 and ΔI_{pk-pk} is the peak to peak AC amplitude. K is the inverse of the total gain constant used in the PPG processing system.

Statistical analysis was performed using the analysis package in Matlab (Mathworks, Inc. Natick, MA). The goodness of model fitting was evaluated with the Sum Square Error (SSE), R-square and the Root Mean Square Error (RMSE). Where SSE shows variation from the mean, R-square is the percentage of the response variable variation, and RMSE is the square root of the variance of the residuals and indicates the absolute fit of the model to the data. Correlation significance is stated with a *p*-value and *t*-value. Pulse Transit Time (PTT) values were calculated as the difference between the location of the peak of the PPG_{AC} signal and the pressure peak. A statistical *t*-test was also performed with values of $p \leq 0.05$ considered to be significant and those where $p < .001$ are highly significant. The slopes (E_v) of the measured and proposed methods were compared using the analysis of the covariance and the percent error values were also calculated with an accepted limit of 5%.

3. Results

3.1. Fluid testing

The prepared hexahydrate cobalt nitrate solution $[Co(OH_2)_6][NO_3]_2$ had a density of 1.091 g/ml, conductivity of 68 mS and acidity of 4 pH at 23 °C. The optical spectra can be seen in Fig. 5 which shows low absorption in the area of interest (660–860 nm). Fluid viscosity tested over a range of shear rates is shown in Table 1.
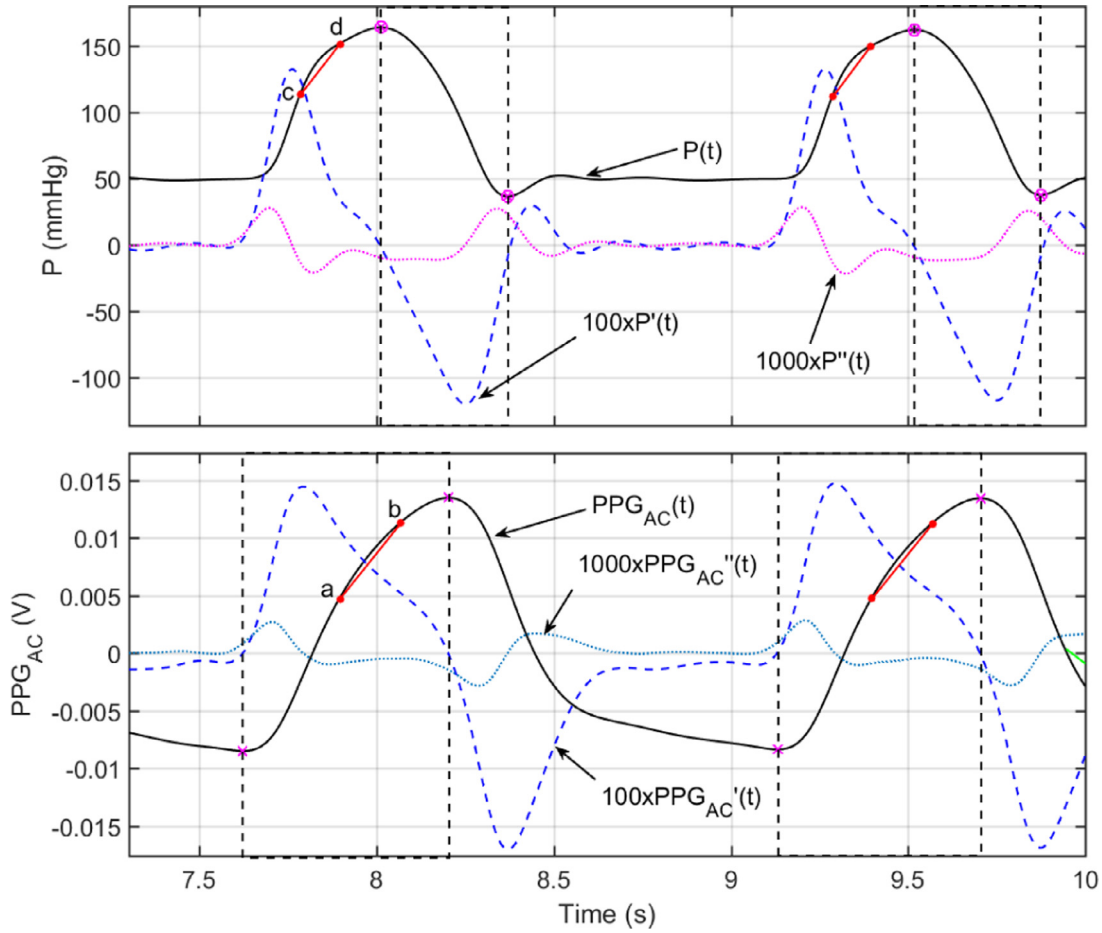
Fig. 4. Three-second snap from the recorded data (stroke volume 70 ml, pump frequency: 0.6 Hz, *Model 1*) portraying the adopted pulse analytics method for pressure and pulsatile Infrared (IR$_{AC}$) PPG signal obtained by a custom made software using Matlab. The highlighted data points were used for the calculation of the slope.
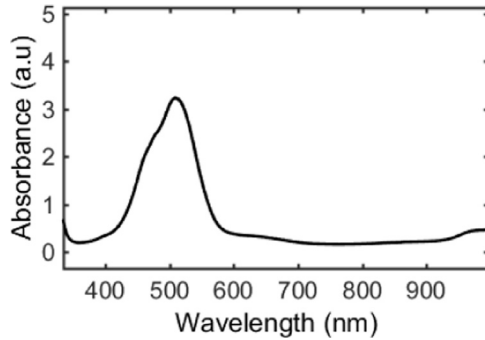

Fig. 5. Optical spectra for the prepared cobalt nitrate solution.

3.2. Effect of pulse frequency PPG and pressure signals

The pump was set to operate at different pulsating frequencies at a constant stroke volume of 30 ml for each model separately. The processed PPG and pressure signals were of high quality. Fig. 6(a) shows a five seconds sample of recorded infrared AC PPG signals and pressure signals from *Model 1* at all operating pulse frequencies ($w1 = 0.6$ Hz, $w2 = 1$ Hz, and $w3 = 1.6$ Hz) at a stroke volume of 30 ml. Fig. 6(b) shows a five seconds sample of recorded infrared AC PPG signals and pressure signals from *Model 2* at all operating pulse frequencies ($w1 = 0.6$ Hz, $w2 = 1$ Hz and $w3 = 1.6$ Hz) at a stroke volume of 30 ml.

3.3. Effect of stroke volume on optical and pressure signals

The pump parameters were altered to increase stroke volume to 70 ml and was set to operate at the same three pulsating frequencies as described in Section 3.2. Fig. 7(a) shows a five seconds sample of recorded infrared AC PPG signals and pressure signals from *Model 1*, at all operating pulse frequencies ($w1 = 0.6$ Hz, $w2 = 1$ Hz, and $w3 = 1.6$ Hz) at a stroke volume of 70 ml. Fig. 7(b) shows a five seconds sample of recorded infrared AC PPG signals and pressure signals from *Model 2*, at all operating pulse frequencies ($w1 = 0.6$ Hz, $w2 = 1$ Hz, and $w3 = 1.6$ Hz) at a stroke volume of 70 ml.

3.4. E$_v$ calculation

This section presents E_v values as calculated from the proposed method for both models. Fig. 8 presents the relationship seen in Eq. (10) for the rate of change of Pressure versus the change rate of NVS. Fig. 8(a) shows values obtained from *Model 1* and Fig. 8(b) shows values obtained from *Model 2*. SSE, R-square, and RMSE values indicate the goodness of the linear fit. Values are obtained from cycle-to-cycle measurements at both stroke volumes (30 ml and 70 ml) and at the three varying pulse frequencies. A plot of residuals versus lagged residuals is presented in Fig. 9 for *Model 1* in Fig. 9(a) and for *Model 2* in Fig. 9(b).
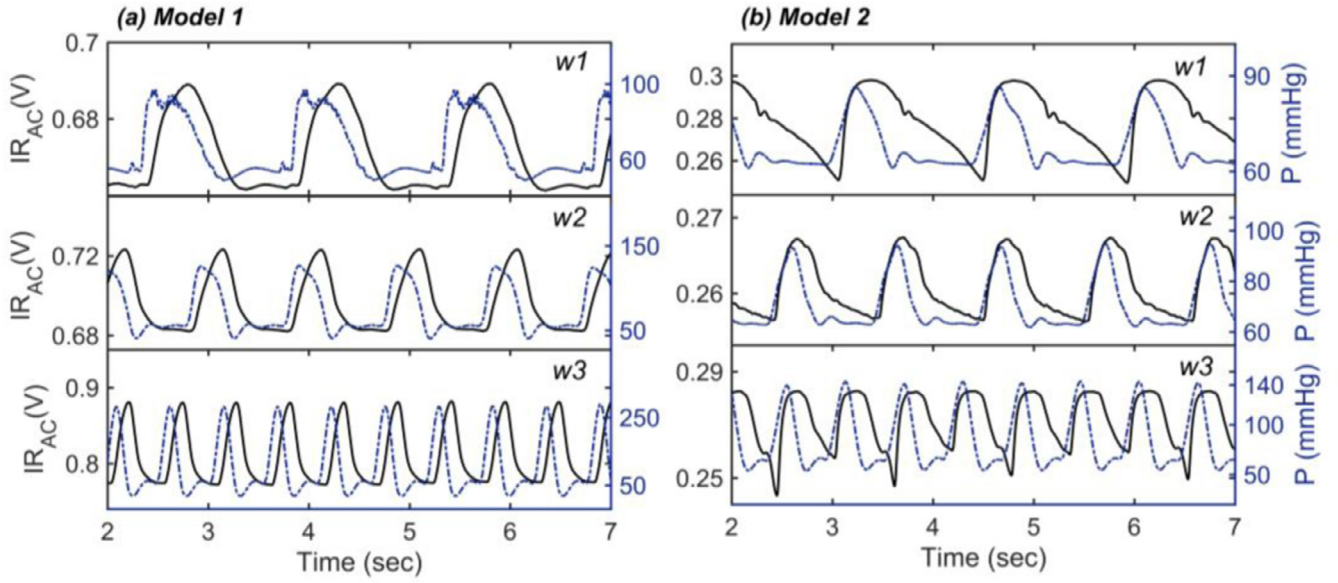
Fig. 6. Five-second sample for Infrared signals (IRAC) acquired from *Model 1* and *Model 2*. Pressure signals (P) are also plotted against the right *y*-axis. This set of data is acquired at 30 ml of stroke volume at all operated pulse frequencies; (a) Signals acquired from *Model 1*.at a stroke volume of 30 ml and all operating frequencies; (b) Shows signals acquired from *Model 2* at a stroke volume of 30 ml and all operating frequencies.

Fig. 7. 5 s sample for Infrared signals (IR$_{AC}$) acquired from *Model 1* and *Model 2*. Pressure signals (P) are also plotted against the right *y*-axis. This set of data is acquired at 70 ml of stroke volume at all operated pulse frequencies; (a) Signals acquired from *Model 1*.at a stroke volume of 70 ml and all operating frequencies; (b) Shows signals acquired from *Model 2* at a stroke volume of 70 ml and all operating frequencies.
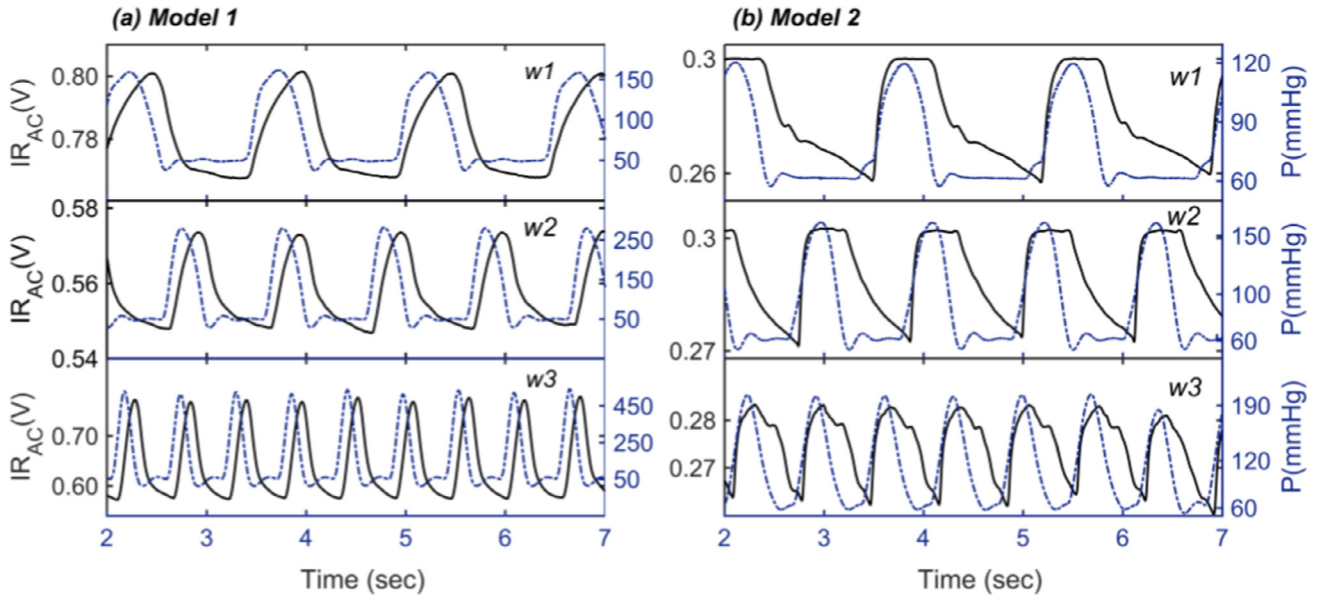
3.5. E$_v$ validation using the gold standard method

The stress-Strain curves for both models as obtained from the gold standard elasticity measurement technique are presented in Fig. 10. Fig. 10(a) shows values obtained from *Model 1*, and Fig. 10(b) shows values obtained for *Model 2*. Elastic Modulus (E) is the slope value obtained using a 1st-degree polynomial fit and E_v is calculated for each model using the formula $E/3(1-2v)$. Where v is the calculated Poisson's ratio and is estimated for each model. The obtained v values for Model 1 and Model 2 were 0.4914 and 0.4884, respectively. SSE, R-square, and RMSE values indicate goodness of the linear approximation fit.

Fig. 10 presents the stress-strain scattergrams as obtained using the gold standard method. A linear approximation is fitted to the data. Fig. 10(a) shows the measured Values for a sample of *Model 1* and Fig. 10(b) shows the measured values for a sample of *Model 2*. Elastic Modulus is the slope of the fitting equation and Volume Elastic Modulus is calculated using the Poisson's ratio. The dotted lines represent the 99% prediction bounds.

The analysis of covariance was performed between the slope of the measured and the validated data, *p*-values for each model. The slope was calculated using all the sampled data and are presented in Table 2.
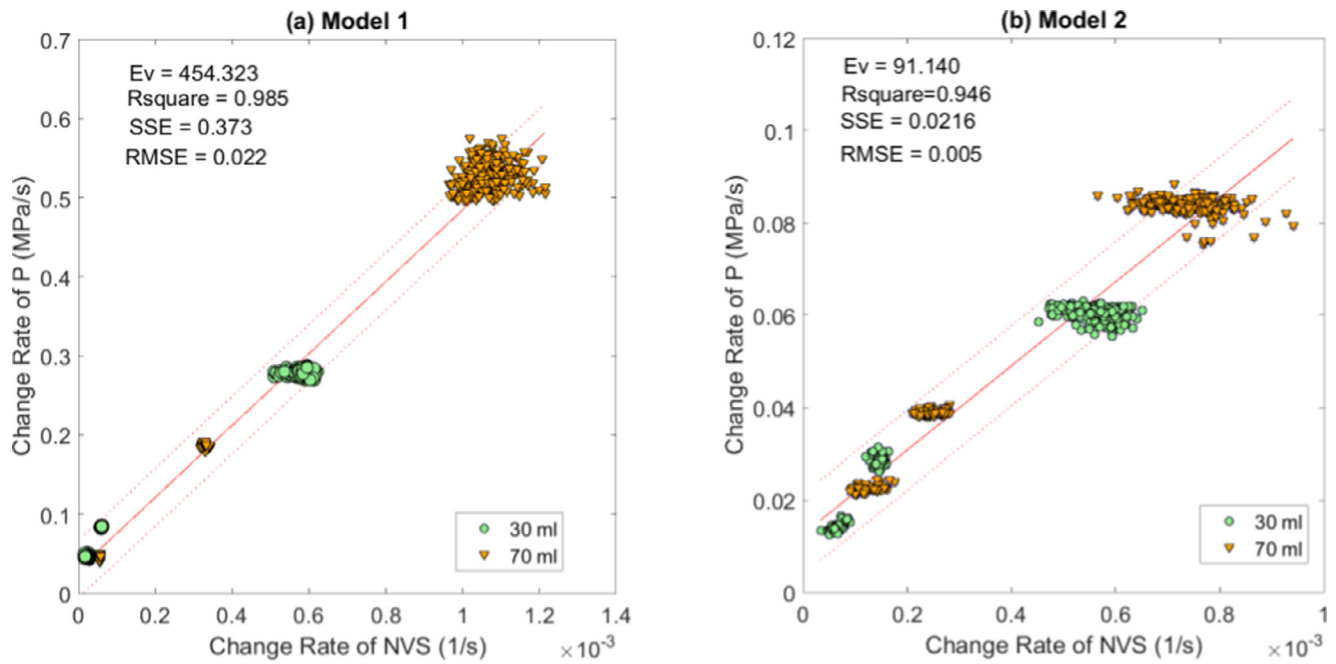
Fig. 8. Scattergrams and linear regression models for the rate of change of Pressure versus the rate of change on Normalised Volumetric Strain; (a) Values obtained from *Model 1*; (b) values obtained from *Model 2*. E_v values are the slope of the fitting equation. R-square, SSE, and RMSE present the goodness of fit. Points are obtained from cycle-to-cycle measurements at both stroke volumes and at varying pumping frequencies.
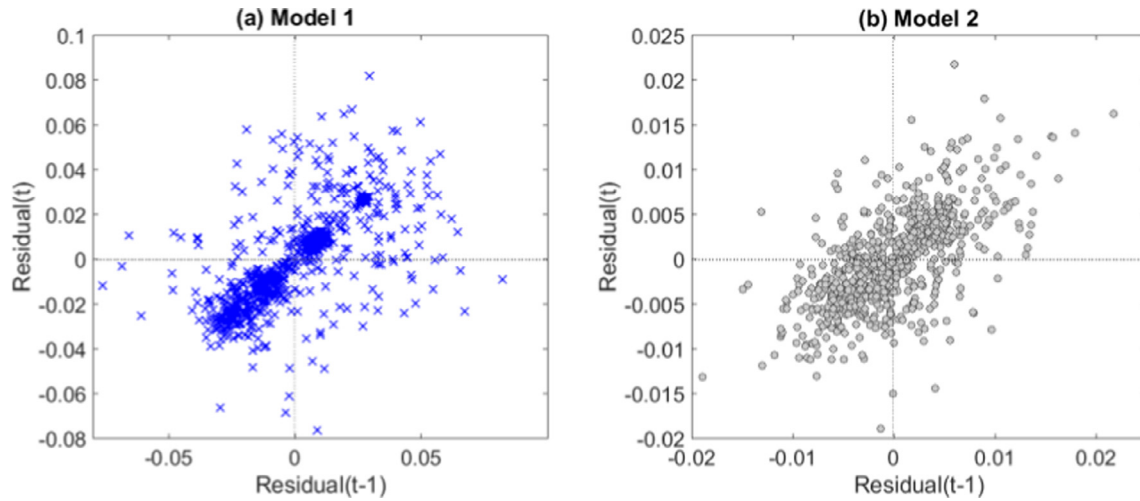

Fig. 9. Plot of residuals versus lagged residuals; (a) *Model 1* and; (b) *Model 2*.

Table 2
Statistical comparison between the proposed method and the gold standard of E_v measurement for *Model 1* and *Model 2*.

Model	p-value	Significant	Percent error (%)
Model 1	.409	**No**	0.258
Model 2	.080	**No**	1.85

3.6. The effect of stroke volume and pulse wave velocity on E_v and PTT

Instantaneous E_v and PTT were calculated at different stroke volumes and at each pumping frequency. Boxplots for the instantaneous E_v and the pulse transit time methods calculated for both models are presented in Fig. 11. Fig. 11(a) shows values for E_v method and Fig. 11(b) shows values for the PTT method. Values

were estimated over 1 min of cycle-to-cycle data at each frequency and stroke volume 70 ml (70), 30 ml (30) and for both models, *Model 1* (M1) and *Model 2* (M2).

In fact, Bonferroni's multiple comparisons tests were able to detect a significant difference between *Model 1* and *Model 2* at both stroke volumes, and at all pumping frequencies from the PTT and E_v methods. However, the PTT method was not able to detect differences at increasing pumping frequencies in *Model 2* from 1 Hz to 1.8 Hz. At a frequency of 1 Hz *Model 2* seemed to produce higher elasticity at higher stroke volumes from the PTT method.

The E_v method showed a consistent significant drop in wall stiffness with increasing pumping frequencies. Moreover, a significant increase in wall stiffness was observed at higher stroke volumes. Nevertheless, this observation diminished at a frequency of 1.8 Hz with no significant difference in E_v values at both stroke volumes. The PTT method still detected significant differences between both stroke volumes at the highest operating frequency.
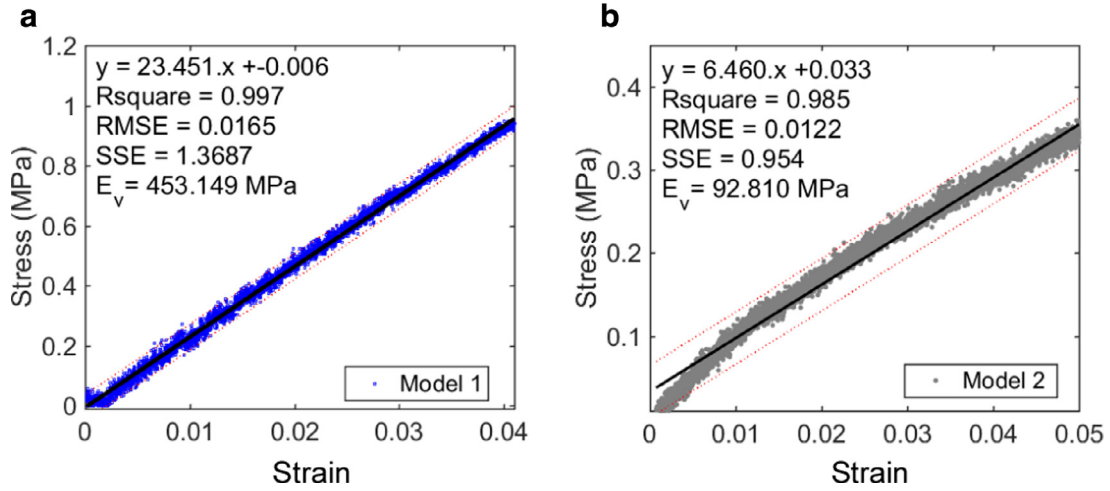
Fig. 10. Stress-strain scattergrams as obtained using the gold standard method, Instron. A linear approximation is fitted to the data; (a) Measured Values for a sample of *Model 1*; (b) Measured values for a sample of *Model 2*.
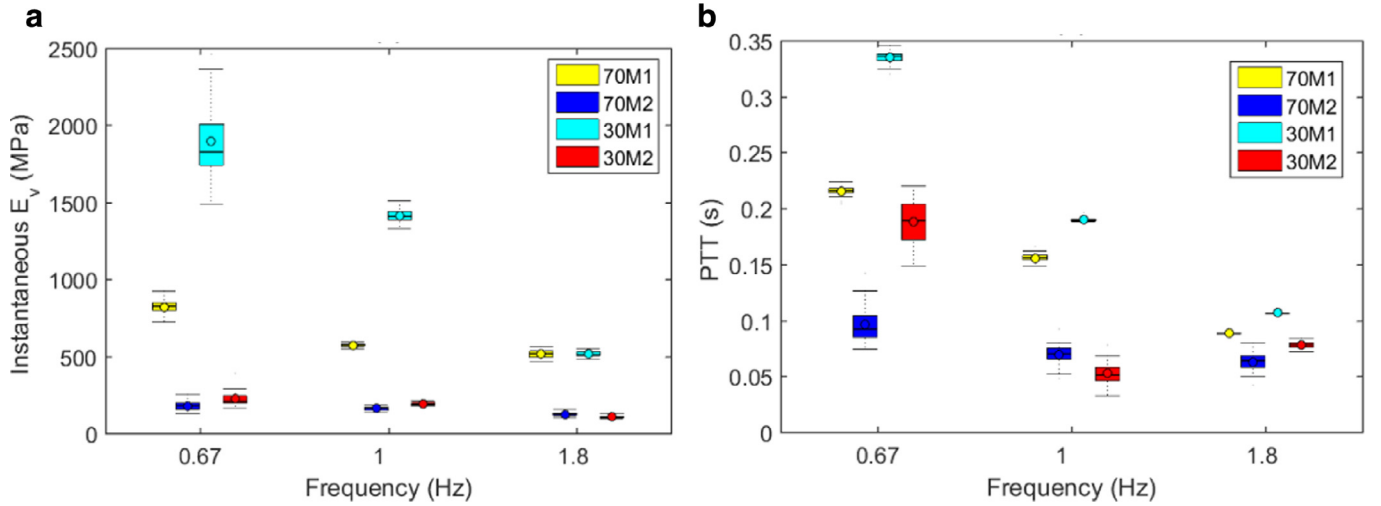

Fig. 11. Boxplots for the instantaneous E_v and the pulse transit time methods calculated for both models at varying pumping frequency are presented in Fig. 11. Panel (a) shows values for E_v method and Panel (b) shows values for the PTT method. Values were estimated over 1 min of cycle-to-cycle data at each frequency and stroke volume, 70 ml (70), 30 ml (30) and for both models, *Model 1* (M1) and *Model 2* (M2).

4. Discussion

An accurate measurement of arterial *volume elastic modulus* can be significant for several medical applications. E_v can provide information on the arterial wall properties regarding the global effect of the circulation. Particularly for our interest, E_v is of great importance as it can be used for the prognosis of CVD at an early stage [10]. Prominently, ATH is directly related to an increase in arterial stiffness [51,52]. This increase in stiffness can be due to two main reasons, the progressive formation of fibrosis, plaque and calcification and hence, increased IMT [11], or the increase in CS and symptomatic hypertension [53]. As these symptoms persist, they can cause further damage and rupture of the arterial wall which can lead to thrombosis and stroke [54,55]. Intervention at an early stage will be life-changing for many patients.

The linear regression was well fitted for *dP/dt* versus the rate of change of *dNVS/dt*. Correlation coefficients were highly significant ($p < .001$) for both models as seen in the scattergrams in Fig. 8. Values from the proposed method for E_v measurement showed agreement with the gold standard Instron elasticity measurement with no significant difference as seen in Fig. 10 and Table 2 and percent errors were within the accepted 5% limit for both models.

These findings highlight that PPG can provide a measure of volumetric strain via the proposed method and hence, using pressure values, an accurate measure of E_v.

4.1. Effect of stroke volume and pumping frequency

It is observed that with increasing pumping frequencies, systolic pressure values and pressure rates increased significantly ($p < .001$) in both models. Systolic pressure values and pressure rates also increased significantly at higher stroke volumes in both models. This is an expected behaviour that is attributed to the increase of pumping powers with increasing pumping frequencies and stroke volumes. When values are compared in both models, it is evident that systolic pressure values and pressure rates are significantly ($p < .001$) higher in *Model 1*, when compared to *Model 2* at the same pumping frequency and stroke volume. This provides further confirmation of the effect of increased AS and IMT on the functionality of the flow, where the affected model (*Model 1*) had a poor response to increased stroke volumes (inertial effects) and pulse frequency (fluid momentum) which caused a much larger increase in transmural pressure values and rates. This also highlights the role of AS in hypertension patients which are linked with ATH and

associated with a risk of lesion rupture [53,56] due to the increase in transmural pressures and circumferential stress. That is to say, the more elastic walls are capable of absorbing fluid energy delivered from the pump, where this energy is reflected back to the fluid and consumed as kinetic energy rather than being dissipated at the wall interface region, causing a significant increase in pressure values as seen in *Model 1*.

The instantaneous E_v values as seen in Fig. 11 highlight that an increase in pumping frequency increase wall stiffness. While Giannattasio et al. observed that AS increase with increasing heart rate [57], Wilkinson et al. also observed an inverse relationship between AIx and heart rates, however, this was possibly caused by the changes in ejection times [58]. While applying such theories to synthetic materials is not completely accurate, from a mechanical point of view, this study agrees with the findings of Giannattasio et al., that wall stiffness in elastic materials increases (drop in distensibility) at increasing pumping frequency due to the concept of stress stiffening, where the stress state (transmural pressure in this case) determines the stiffening of the wall. While these observations were consistent and significant in both models via the Instantaneous E_v method, the PTT method was able to detect this behaviour in *Model 1*, nevertheless, there was no significant difference observed in *Model 2* when the frequency increased to 1.8 Hz at both stroke volumes. Though this behaviour is not clear, it might be possible that the fluid wave velocity reached its maximum at 1 Hz, and the phase between pressure and volumetric strain signals did not change. The PTT method does not directly account pressure or stress values and hence our suggestion that it might be inaccurately interpreted in some cases.

At low pumping frequencies, the effect of stroke volume seemed to be significant, with higher wall stiffness values observed at lower stroke volumes. The effect of stroke volume diminished at higher pumping frequencies, where at 1.8 Hz, both Instantaneous E_v values had no significant difference. Yet, the PTT method was still able to detect a significant difference in values between both stroke volumes at the highest frequency. With increasing frequencies, fluid viscosity drops significantly (see Table 1), and hence fluid inertia becomes an insignificant factor in the dynamics of the flow. However, the change of fluid characteristics might allow the pulsatile fluid signal to travel at a higher speed in the axial direction, and hence, the drop in phase between pressure and PPG signals might not be due to changes in wall stiffness. These findings highlight that as the E_v and the PTT methods were able to detect changes in arterial stiffness between both models, E_v provides a direct quantification of arterial stiffness and might provide better accuracy even at an increased pumping frequency or stroke volume changes.

4.2. Remarks on the origin of the PPG

It is usually known that the PPG signal behaves inversely in relation to blood pressure and it should be inverted to correlate positively with the blood volume. Recently, Teplov et al. reported the coexistence of two mutually inverted signals in adjacent locations [59]. This behaviour was also observed in this investigation, as inverted signals were observed along the same tube in different locations, and it is possibly related to the sensor contact pressure during the wall movement or the direction of the flow. Nevertheless, this issue does not affect the amplitude or the morphology of the signal and is not the main concern of this work. To avoid any errors related to the inversion of the PPG signal, the signals were normalised to correlate with the blood pressure signal. As PPG and pressure signals were recorded simultaneously, the peak of the PPG signal was determined in relation to the pressure peak in each cycle.

Finally, this study highlights the suitability of photoplethysmography to provide a normalised measure of volume and hence volumetric strain. Recent studies have highlighted the dependency of PPG on wall elasticity and suggested that the source of modulation of the PPG is the elastic deformations of the dermis as an alternative model of the light modulation, not the arterial blood volumetric changes. In fact, this theory sheds light on the importance of wall elasticity in the formation of the PPG, however, it dismisses a major factor in the formation of the PPG which is fluid volume and radial stresses. This study directs the attention to consider the PPG as strain volumetric changes, a measure dependent on wall elasticity and radial stresses. Radial stresses are affected by the momentum of the fluid (e.g. changing pumping frequency) and by fluid inertia (e.g. the effect of stroke volumes). In order to further study the PPG signal, factors affecting the volume elastic modulus and transmural pressures must be considered.

4.3. Study limitations

Our study confirms the capability of both PPG and pressure signals to provide an accurate and direct measure of AS by E_v quantification. Nevertheless, the study incurs some limitations that need to be considered before it can be applied in an *in vivo* investigation.

The main limitation is the nature of the study, meaning *in vitro*. The developed *in vitro* model was only a tool to provide a proof of concept, hence, only the arterial component of the system was presented and the compliance, single diameter and blood oxygenation are limiting factors. PPG signals obtained *in vivo* will contain physiological information related to respiration, temperature changes, nitric oxide release, vasoconstriction and dilation, amongst others. Hence, an effective and systematic PPG decomposition technique together with rigorous *in vivo* studies will be required in order to isolate and account the contributions of such parameters on the PPG signal.

The basic assumption for the derivation equations considers the fluid as constitutes and non-scattering homogeneous medium. However, this presumption is not valid for blood suspension because the light interaction through the suspension is caused by absorption, as well as scattering events [60]. Nonetheless, the evidence is accumulating that Beer-Lambert's law can be extended to a light scattering system [61]. The derivation can be expanded to consider such factors.

The factors which can violate the directly proportional relationship between V_o were not investigated experimentally in this study (c and ε). Yet, during an *in vivo* setup, ε is constant within and between subjects due to the fixed absorption coefficients of oxy and deoxyhaemoglobin at the specific wavelength. In respect to c, hematocrit changes are expected to be only a few percent different due to changes in neurohormonal factors.

One of the limitations of this study is also the use of an invasive pressure measurement method via a catheter transducer. We suggest the utilisation of emerging real-time and non-invasive methods for blood pressure monitoring (i.e. Finapres, CNAP or Nexfin) to overcome this limitation.

Despite the limitations, our method was able to provide a direct measurement of E_v with a marginal error when compared to the gold standard method without the need for knowledge of geometrical dimensions, which makes it a potential method for further *in vivo* studies that should investigate different healthy and diseased cases to demonstrate the potential of the method. Such approach will pave the way for further non-invasive applications in sensing systems for continuous monitoring of arterial stiffness. Potentially, this method can bring many benefits to the clinical sector and particularly CVD patients.

5. Conclusion

In this manuscript, we demonstrated the capability of the PPG to provide a measure of volumetric strain through NVS, which is utilised to measure E_v as a potential method for direct quantification of arterial stiffness. We have evaluated our method in an *in vitro* model of a healthy artery and another of an artery affected with ATH. We further explored our method under conditions of increased stroke volumes and pulse frequencies. Experimental results are in strong agreement with the gold standard measurement of E_v. The study provides a proof of concept for direct measurement of AS under simulated conditions for hypotensive, normotensive and hypertensive scenarios and paves the way for a potential *in vivo* non-invasive and continuous method for direct measurement of E_v using PPG.

References

[1] Members AF, et al. European guidelines on cardiovascular disease prevention in clinical practice (version 2012). Eur. Heart J. 2012;33(13):1635–701.

[2] Cavender MA, et al. Impact of diabetes on hospitalization for heart failure, cardiovascular events, and death: outcomes at 4 years from the REACH registry. *Circulation*, p. CIRCULATIONAHA. 2015;114:014796.

[3] Daviglus ML, GA T, Avilés-Santa M, et al. Prevalence of major cardiovascular risk factors and cardiovascular diseases among hispanic/latino individuals of diverse backgrounds in the united states. JAMA 2012;308(17):1775–84.

[4] O'Rourke MF, Staessen JA, Vlachopoulos C, Duprez D, érard G, Plante E. Clinical applications of arterial stiffness; definitions and reference values. Am. J. Hypertens. 2002;15(5):426–44.

[5] de O Alvim R, et al. Impact of diabetes mellitus on arterial stiffness in a representative sample of an urban Brazilian population. Diabetol. Metab. Syndr. 2013;5(1):45.

[6] Safar ME, Levy BI, Struijker-Boudier H. Current perspectives on arterial stiffness and pulse pressure in hypertension and cardiovascular diseases. Circulation 2003;107(22):2864–9.

[7] Rehill N, Beck CR, Yeo KR, Yeo WW. The effect of chronic tobacco smoking on arterial stiffness. Br. J. Clin. Pharmacol. 2006;61(6):767–73.

[8] Zebekakis PE, et al. Obesity is associated with increased arterial stiffness from adolescence until old age. J. Hypertens. 2005;23(10):1839–46.

[9] De Groot E, et al. Measurement of arterial wall thickness as a surrogate marker for atherosclerosis. Circulation 2004;109(23):III33–8.

[10] Cecelja M, Chowienczyk P. Role of arterial stiffness in cardiovascular disease. JRSM Cardiovasc. Dis. 2012;1(4):11.

[11] Wentzel JJ, et al. Extension of increased atherosclerotic wall thickness into high shear stress regions is associated with loss of compensatory remodeling. Circulation 2003;108(1):17–23.

[12] Matsushima Y, et al. Relationship of carotid intima-media thickness, pulse wave velocity, and ankle brachial index to the severity of coronary artery atherosclerosis. Clin. Cardiol. 2004;27(11):629–34.

[13] Lee RT, Schoen FJ, Loree HM, Lark MW, Libby P. Circumferential stress and matrix metalloproteinase 1 in human coronary atherosclerosis implications for plaque rupture. Arterioscler. Thromb. Vasc. Biol. 1996;16(8):1070–3.

[14] Cheng GC, Loree HM, Kamm RD, Fishbein MC, Lee RT. Distribution of circumferential stress in ruptured and stable atherosclerotic lesions. A structural analysis with histopathological correlation.. Circulation 1993;87(4):1179–87.

[15] Duprez DA. Is vascular stiffness a target for therapy? Cardiovasc. Drugs Ther. Spons. Int. Soc. Cardiovasc. Pharmacother. 2010;24(4):305–10.

[16] Janic M, Lunder M, Sabovic M. Arterial stiffness and cardiovascular therapy. Bio. Med. Res. Int. 2014;2014:e621437.

[17] Njoum H, Kyriacou PA. Photoplethysmography for the assessment of haemorheology. Sci. Rep. 2017;7(1):1406.

[18] Njoum H, Kyriacou PA. Photoplethysmography for an independent measure of pulsatile pressure under controlled flow conditions. Physiol. Meas. 2017;38(2):87.

[19] Tanaka G, et al. A novel photoplethysmography technique to derive normalized arterial stiffness as a blood pressure independent measure in the finger vascular bed. Physiol. Meas. 2011;32(11):1869.

[20] Clarenbach CF, et al. Comparison of photoplethysmographic and arterial tonometry-derived indices of arterial stiffness. Hypertens. Res. Off. J. Jpn. Soc. Hypertens. 2012;35(2):228–33.

[21] Bortolotto LA, Blacher J, Kondo T, Takazawa K, Safar ME. Assessment of vascular aging and atherosclerosis in hypertensive subjects: second derivative of photoplethysmogram versus pulse wave velocity. Am. J. Hypertens. 2000;13(2):165–71.

[22] Severinghaus JW. Takuo aoyagi: discovery of pulse oximetry. Anesth. Analg. 2007;105(6S):S1–4 Suppl.

[23] Nijboer JA, Dorlas JC, Mahieu HF. Photoelectric plethysmography–some fundamental aspects of the reflection and transmission method. Clin. Phys. Physiol. Meas. 1981;2(3):205–15.

[24] Kyriacou PA. Direct pulse oximetry within the esophagus, on the surface of abdominal viscera, and on free flaps:. Anesth. Analg. 2013;117(4):824–33.

[25] Shelley KH. Photoplethysmography: beyond the calculation of arterial oxygen saturation and heart rate. Anesth. Analg. 2007;105(6):S31–6.

[26] Lindberg LG, Tamura T, Öberg PPÅ. Photoplethysmography. Med. Biol. Eng. Comput. 1991;29(1):40–7.

[27] Kamal AAR, Harness JB, Irving G, Mearns AJ. Skin photoplethysmography — a review. Comput. Methods Programs Biomed. 1989;28(4):257–69.

[28] D'Agrosa LS, Hertzman AB. Opacity pulse of individual minute arteries. J. Appl. Physiol. 1967;23(5):613–20.

[29] Sommermeyer D, Schwaibold M, Schöller B, Grote L, Hedner J, Bolz A. Prediction of cardiovascular risk from peripheral pulse wave. In: Dössel O, Schlegel WC, editors. Proceedings of the World Congress on Medical Physics and Biomedical Engineering. Springer; 2009. p. 891–2.

[30] Njoum H. Investigation of finger reflectance photoplethysmography in volunteers undergoing a local sympathetic stimulation. J. Phys. Conf. Ser. 2013;450(1):012012.

[31] Ruiz-Rodríguez JC, et al. Innovative continuous non-invasive cuffless blood pressure monitoring based on photoplethysmography technology. Intensive Care Med 2013;39(9):1618–25.

[32] Buclin T, Buchwalder-Csajka C, Brunner HR, Biollaz J. Evaluation of noninvasive blood pressure recording by photoplethysmography in clinical studies using angiotensin challenges. Br. J. Clin. Pharmacol. 1999;48(4):586–93.

[33] Teng XF, Zhang YT. Continuous and noninvasive estimation of arterial blood pressure using a photoplethysmographic approach. In: Proceedings of the 25th Annual International Conference of the IEEE Engineering in Medicine and Biology Society, 4; 2003. p. 3153–6.

[34] Nakajima K, Tamura T, Miike H. Monitoring of heart and respiratory rates by photoplethysmography using a digital filtering technique. Med. Eng. Phys. 1996;18(5):365–72.

[35] Alian AA, Shelley KH. Respiratory physiology and the impact of different modes of ventilation on the photoplethysmographic waveform. Sensors 2012;12(2):2236–54.

[36] Pannier BM, Avolio AP, Hoeks A, Mancia G, Takazawa K. Methods and devices for measuring arterial compliance in humans. Am. J. Hypertens. 2002;15(8):743–53.

[37] Naidu MUR, Reddy BM, Yashmaina S, Patnaik AN, Rani PU. Validity and reproducibility of arterial pulse wave velocity measurement using new device with oscillometric technique: a pilot study. Biomed. Eng. OnLine 2005;4:49.

[38] Jerrard-Dunne P, Mahmud A, Feely J. Ambulatory arterial stiffness index, pulse wave velocity and augmentation index – interchangeable or mutually exclusive measures?:. J. Hypertens. 2008;26(3):529–34.

[39] Nürnberger J, Keflioglu-Scheiber A, Opazo Saez AM, Wenzel RR, Philipp T, Schäfers RF. Augmentation index is associated with cardiovascular risk. J. Hypertens. 2002;20(12):2407–14.

[40] Rajzer MW, Wojciechowska W, Klocek M, Palka I, Brzozowska-Kiszka M, Kawecka-Jaszcz K. Comparison of aortic pulse wave velocity measured by three techniques: Complior, SphygmoCor and Arteriograph. J. Hypertens. 2008;26(10):2001–7.

[41] Miyatani M, Masani K, Oh PI, Miyachi M, Popovic MR, Craven BC. Pulse wave velocity for assessment of arterial stiffness among people with spinal cord injury: a pilot study. J. Spinal Cord Med. 2009;32(1):72–8.

[42] Millasseau SC, Ritter JM, Takazawa K, Chowienczyk PJ. Contour analysis of the photoplethysmographic pulse measured at the finger:. J. Hypertens. 2006;24(8):1449–56.

[43] Takazawa K, et al. Assessment of vasoactive agents and vascular aging by the second derivative of photoplethysmogram waveform. Hypertension 1998;32(2):365–70.

[44] Obata Y, et al. The effects of hemodynamic changes on pulse wave velocity in cardiothoracic surgical patients. BioMed Res. Int. 2016;2016.

[45] Nürnberger J, Dammer S, Opazo Saez A, Philipp T, Schäfers RF. Diastolic blood pressure is an important determinant of augmentation index and pulse wave velocity in young, healthy males. J. Hum. Hypertens. 2003;17(3):153–8.

[46] Kamoi S, et al. Relationship between stroke volume and pulse wave velocity. IFAC-Pap 2015;48(20):285–90.

[47] Steppan J, Barodka V, Berkowitz DE, Nyhan D. Vascular stiffness and increased pulse pressure in the aging cardiovascular system. Cardiology Res. Pract. 2011. [Online]. Available https://www.hindawi.com/journals/crp/2011/263585/ [Accessed: 10-Nov-2017].

[48] Zureik M, et al. Carotid plaques, but not common carotid intima-media thickness, are independently associated with aortic stiffness. J. Hypertens. 2002;20(1):85–93.

[49] Zamir M. The Physics of Pulsatile Flow. Springer; 2000.

[50] Sawada Y, Tanaka G, Yamakoshi K. Normalized pulse volume (NPV) derived photo-plethysmographically as a more valid measure of the finger vascular tone. Int. J. Psychophysiol. 2001;41(1):1–10.

[51] Oliver JJ, Webb DJ. Noninvasive assessment of arterial stiffness and risk of atherosclerotic events. Arterioscler. Thromb. Vasc. Biol. 2003;23(4):554–66.

[52] Aggoun Y, Szezepanski I, Bonnet D. Noninvasive assessment of arterial stiffness and risk of atherosclerotic events in children. Pediatr. Res. 2005;58(2):173–8.

[53] Alexander RW. Hypertension and the pathogenesis of atherosclerosis oxidative stress and the mediation of arterial inflammatory response: a new perspective. Hypertension 1995;25(2):155–61.

[54] Mitchell GF, et al. Arterial stiffness and cardiovascular events the framingham heart study. Circulation 2010;121(4):505–11.

[55] Mattace-Raso FUS, et al. Arterial stiffness and risk of coronary heart disease and stroke the rotterdam study. Circulation 2006;113(5):657–63.

[56] Hollander W. Role of hypertension in atherosclerosis and cardiovascular disease. Am. J. Cardiol. 1976;38(6):786–800.

[57] Giannattasio C, et al. Effects of heart rate changes on arterial distensibility in humans. Hypertension 2003;42(3):253–6.

[58] Wilkinson IB, MacCallum H, Flint L, Cockcroft JR, Newby DE, Webb DJ. The influence of heart rate on augmentation index and central arterial pressure in humans. J. Physiol. 2000;525:263–70.

[59] Teplov V, Nippolainen E, Makarenko AA, Giniatullin R, Kamshilin AA. Ambiguity of mapping the relative phase of blood pulsations. Biomed. Opt. Express 2014;5(9):3123.

[60] Friebel M, Roggan A, Müller G, Meinke M. Determination of optical properties of human blood in the spectral range 250 to 1100 nm using Monte Carlo simulations with hematocrit-dependent effective scattering phase functions. J. Biomed. Opt. 2006;11(3):034021.

[61] Kocsis L, Herman P, Eke A. The modified Beer–Lambert law revisited. Phys. Med. Biol. 2006;51(5):N91.